Original article

Quercetin mitigates the adverse effects of high fat diet on pancreatic and renal tissues in adult male albino rats

Rabab Ahmed Rasheed [a,*], Mohamed S. Elshikh [b], Mohamed Othman Mohamed [c], Mohamed Faisal Darweesh [d], Dina S. Hussein [e], Saeedah Musaed Almutairi [b], Azza Saleh Embaby [f]

[a] Histology & Cell Biology Department, Faculty of Medicine, King Salman International University, South Sinai, Egypt
[b] Department of Botany and Microbiology, College of Science, King Saud University, P.O. 2455, Riyadh 11451, Saudi Arabia
[c] Anatomy Department, Faculty of Medicine, King Salman International University, South Sinai, Egypt
[d] Pathology Department, Faculty of Medicine, King Salman International University, South Sinai, Egypt
[e] Department of Chemistry, College of Sciences and Health, Cleveland State University, Cleveland 44115, United States
[f] Medical Histology & Cell Biology Department, Faculty of Medicine, Beni-Suef University, Beni-Suef, Egypt

A R T I C L E   I N F O

A B S T R A C T

Objectives: Obesity as a consequence of high fat diet (HFD) has become an uprising major global health problem with multiorgan affection. Quercetin proved a unique ameliorative potential against hazards of HFD.

Methods: Forty rats were divided into four groups. Group I: Control group (10% of energy from fat). Group II: (10% of energy from fat +50 mg/kg quercetin). Group III: (60% of energy from fat). Group IV: (60% of energy from fat +50 mg/kg quercetin). After12 weeks, all rats were sacrificed, kidney and pancreas were taken and processed for H&E, Mallory's trichrome stains and immunohistochemical examination.

Results: Both pancreatic and renal tissues showed histopathological degenerative and inflammatory changes in group III that was markedly improved in group IV treated with quercetin. Concerning the mean area percent of collagen fibers and Bcl-2 expression in both renal and pancreatic tissues that showed a highly significant difference in group III ($p < 0.001$) as compared to all other groups and a highly significant difference ($p < 0.001$) in group IV compared to group III.

Conclusion: These results confirmed the negative influence of HFD intake on both renal and pancreatic tissues and the protective effect of concomitant use of quercetin. Quercetin's therapeutic potential for metabolic disorders may become more evident and widely accepted.

1. Introduction

Diet has important effects on normal physiology, and the potential deleterious effects of high-fat diets (HFD) and obesity on health are being increasingly described (Jarvis et al., 2020). Obesity, which reaches an epidemic, is characterized by alterations in metabolic and hormonal profiles (Matuszewska et al., 2020). Obesity and dietary fat are significant causes of several health issues such as dyslipidemia, type II diabetes, heart, renal and respiratory diseases (Kovesdy et al., 2017; Shirai et al., 2016). HFD intake can lead to alterations in the exocrine and endocrine pancreas (Zhang et al., 2008), indicating that HFD is associated with chronic pancreas injuries. Intake of a high-fat, high-sucrose diet not only results in weight gain but also increases steatosis and inflammatory cell infiltrates in the pancreas of mice and rats (Cao et al., 2014). Glucolipotoxicity associated with chronic over-nutrition leads to overproduction of ROS (Reactive Oxygen Species) in several body tissues, including pancreatic β-cells. The oxidative stress that occurs in this prediabetic environment is thought to have a role in β-cell dysfunction. Currently, there is a great need for treatment strategies that interrupt the pathogenesis of β-cells dysfunction to preserve a functional β-cell mass and thus prevent the development and progression of Type 2 Diabetes Mellitus (T2DM)

* Corresponding authors.

E-mail addresses: rasheedrabab@gmail.com, rabab.rasheed@ksiu.edu.eg (R.A. Rasheed), melshikh@ksu.edu.sa (M.S. Elshikh), mohammed.darweesh@ksiu.edu.eg (M.F. Darweesh), d.husseinabdelwahab@vikes.csu.ohio.edu (D.S. Hussein), alsaeedah@ksu.edu.sa (S.M. Almutairi).

Rabab Ahmed Rasheed, M.S. Elshikh, Mohamed Othman Mohamed et al.

Journal of King Saud University – Science 34 (2022) 101946

(Madduma et al., 2020). In the same context, chronic low-grade inflammation is a significant stimulus for the progression of chronic kidney disease (CKD) in individuals consuming a high-fat diet (HFD) (Ježek et al., 2019).

CKD has emerged as a serious economic threat to health care systems globally due to its increasing prevalence, complications (such as anemia, cardiovascular disease, bone, and mineral disorders), immense expenses associated with renal replacement therapy, high morbidity, and mortality (Yang et al., 2017). It was reported that inflammatory stress promoted renal lipid accumulation and glomerular lesion formation in high-fat diet-fed obese mice that displayed renal and systemic changes compatible with human obesity-related CKD (Zoccali et al., 2017). Lipids may play a major role in the development of renal tissue damage (Dominguez et al., 2000). Several possible pathways for renal injury have been postulated, including oxidative damage, the generation of ROS and lipid peroxidation (Muñoz-García et al., 2009). Quercetin (QE) is a flavonoid commonly found in frequently consumed foods, including apples, berries, onion, tea, nuts, seed, and vegetables that represent an integral part of the human diet. QE has biological, pharmacological, and therapeutic characteristics, which are thought to stem from its antioxidant capabilities (Perez-Vizcaino et al., 2009). QE is a natural antioxidant with various biological activities including scavenging free radicals and inhibiting xanthine oxidase and lipid peroxidation (Al-Rasheed et al., 2013). Over the past few decades, different studies have focused on the therapeutic properties of QE for diabetes, cardiovascular diseases, kidney diseases, neurodegenerative disorders, reproductive dysfunction, and cancer (Shi et al., 2019).

An increasing number of studies have evaluated the beneficial effects of QE on the treatment of diabetes (Yang and Kang, 2018). Observed complications resulting from QE intervention have been significantly decreased (Shi et al., 2019). The current study aimed to evaluate the same effect histologically and immunohistochemically on kidney and pancreas of adult male albino rats, since most previous studies concerned HFD impact on both kidney and pancreas and the possible protective role of QE, were based on clinical and biochemical effects.

2. Materials and methods

2.1. Chemicals

Quercetin was purchased from Sigma-Aldrich, the USA, as quercetin hydrate ≥95% purity in powder form [product Number 337951, pack size: 100 gm].

2.2. Experimental animals

In accordance with Beni–Suef University Animal Use Committee guidelines (Approval number 170/3rd Nov. 2019), forty adult male albino rats aged from ten to twelve weeks, with average weight ranging from 150 to 180 gm, were housed in the Animal House of Faculty of Medicine, Beni–Suef University, Beni–Suef, Egypt. Rats were kept in a sanitary environment within a temperature range (22–24 °C) and light-controlled room on an alternating 12:12 h light–dark, fed ad libitum with unrestricted access to tap water. They were given one week to acclimate before to the experiment.

2.3. Experimental design

The rats were randomly distributed in isolated well aerated propylene cages with metal mesh covers containing five rats each. The rats were divided equally into four groups, ten rats each, and

for a total duration of twelve weeks according to (Madduma et al., 2020; Zhang et al., 2020):

Group I (Control, n = 10): received standard diet (composed of 13.5% of fat, 61.3% of carbohydrate and 25.2% of protein, based on the total energy content of 2830 kcal/kg) (Ternacle et al., 2017; Yi et al., 2020).

Group II (QE, n = 10): received standard diet and quercetin (50 mg/kg b.wt) (Mzhelskaya et al., 2020; Mzhelskaya et al., 2019).

Group III (HFD, n = 10): received HFD (composed of 60% of fat, 20% of carbohydrate, and 20% of protein). Every gram of its ingredient contained 5.24 kcal, including 232 mg cholesterol, based on the total energy content of 5243 kcal/kg (Ternacle et al., 2017; Park et al., 2020).

Group IV (HFDQ, n = 10): received HFD and quercetin (50 mg/kg b.wt) daily.

By the end of the twelfth week, all rats were sacrificed by an overdose of anesthesia (100 mg/kg ketamine-xylazaine IP) (Shaw and Harper, 2013; Ko et al., 2019).

2.4. Measurement of body weights and relative organs' weights

Rats of all groups were weighed at the start and at the end of the experiment. The initial and final body weights were recorded. Determination of the percent rise in body weight (% B.Wt gain) throughout the experiment was done using this formula: = (final body weight − initial body weight) / final body weight × 100. The relative pancreas and kidney weights in all rats of all groups were measured and recorded according to this formula: = (organ weight / final body weight) × 100. (Ekeleme-Egedigwe et al., 2017).

2.5. Histological studies

Samples from the pancreata and kidneys from all rats of all groups were dissected then fixed in 10% formalin solution and paraffin-embedded. 6 μm thick sections were obtained and processed for staining with hematoxylin and eosin, and Mallory's trichrome to reveal collagen fibers (Suvarna et al., 2013; Kiernan, 2015). Immunohistochemical stain using avidin–biotin-peroxidase system was used for the detection of Bcl-2 as an anti-apoptotic protein (CAS No. 85878, Sigma-Aldrich, Steinheim, Germany) using a primary antibody (rabbit polyclonal antibody) (product No. LS-C78828; Life span Biosciences, Inc. Seattle, WA, USA) and then incubated with secondary anti-rabbit antibody (Zymed Laboratories). The staining was accomplished with diaminobenzidine (DAB) according to (Ramos-Vara and Miller, 2014).

2.6. Morphometric study

Ten haphazardly-picked non-overlapping fields from different sections of pancreata and kidneys of all studied groups were used to define the mean area percent of collagen fibers in Mallory's trichrome stained sections and Bcl-2 expression in immunostained sections. Measurements were performed and gathered at King Salman International University, Faculty of Medicine, using image analysis computer system Ltd. with Leica Qwin-500 LTD-software (Cambridge, England).

2.7. Statistical analysis

The Statistical Package of Social Science (SPSS) (ver 26) generated the results. Data were summarized as mean ± standard deviation (SD). One-way analysis of variance (ANOVA) was used to compare the results across the different study groups, followed by a "Tuckey" post-hoc test to determine statistical significance.

Rabab Ahmed Rasheed, M.S. Elshikh, Mohamed Othman Mohamed et al.

Journal of King Saud University – Science 34 (2022) 101946

(P-value was considered significant if <0.05 and highly significant if <0.001) (Emsley et al., 2010).

3. Results

No deaths were observed in all rats.

3.1. Results of weight gain:

Rats of HFD group showed increased final body weight and relative organs' weight when compared to control and QE groups. This was observed from second week, until the end of the experimental period. The values of initial, final, relative pancreas and kidney weights are shown as mean ± standard deviation in Table 1 and Histogram 1.

3.2. Histological results of hematoxylin and eosin-stained sections

3.2.1. Pancreatic tissue examination

Control and QE groups showed typical pancreatic lobules alienated by delicate interlobular septa containing blood vessels, lobules were formed of crowded acini lined by pyramidal cells with basal vesicular nuclei, apical acidophilic zymogen granules and basal basophilic cytoplasm, normally looking pale scattered islets of Langerhans composed of clusters of hormone secreting cells with intervening fenestrated capillaries in between the islet cells, intralobular ducts lined by simple cubical epithelium with centroacinose cell were spotted (Fig. 1 A&B respectively). HFD group showed various islet and acinar lesions. The islets' lesion appeared as shredded islets with irregular contour, reduced islet cells' mass with vacuolated cytoplasm, pyknotic and karyolitic nuclei. Many cells were disrupted and degenerated. The islets' blood sinusoids were significantly dilatated and congested. The blood vessels were congested as well (Fig. 1C). The acinar lesions were demonstrated as heavy inflammatory cellular infiltrates invaded the pancreatic lobules around the ducts and blood vessels, and distorted acini with reparative attempts. Several pyknotic nuclei were spotted. The intralobular and interlobular ducts were dilated with retained secretions in their lumina. The interlobular septae were widened and contained markedly congested blood vessels. The wall of blood vessels was thickened with eosinophilic hyaline material. Large deposits of hyaline material could be obviously seen intracellular and in between the acini. Fatty infiltration is detected adjacent to ducts and blood vessels (Fig. 1 D,E&F).
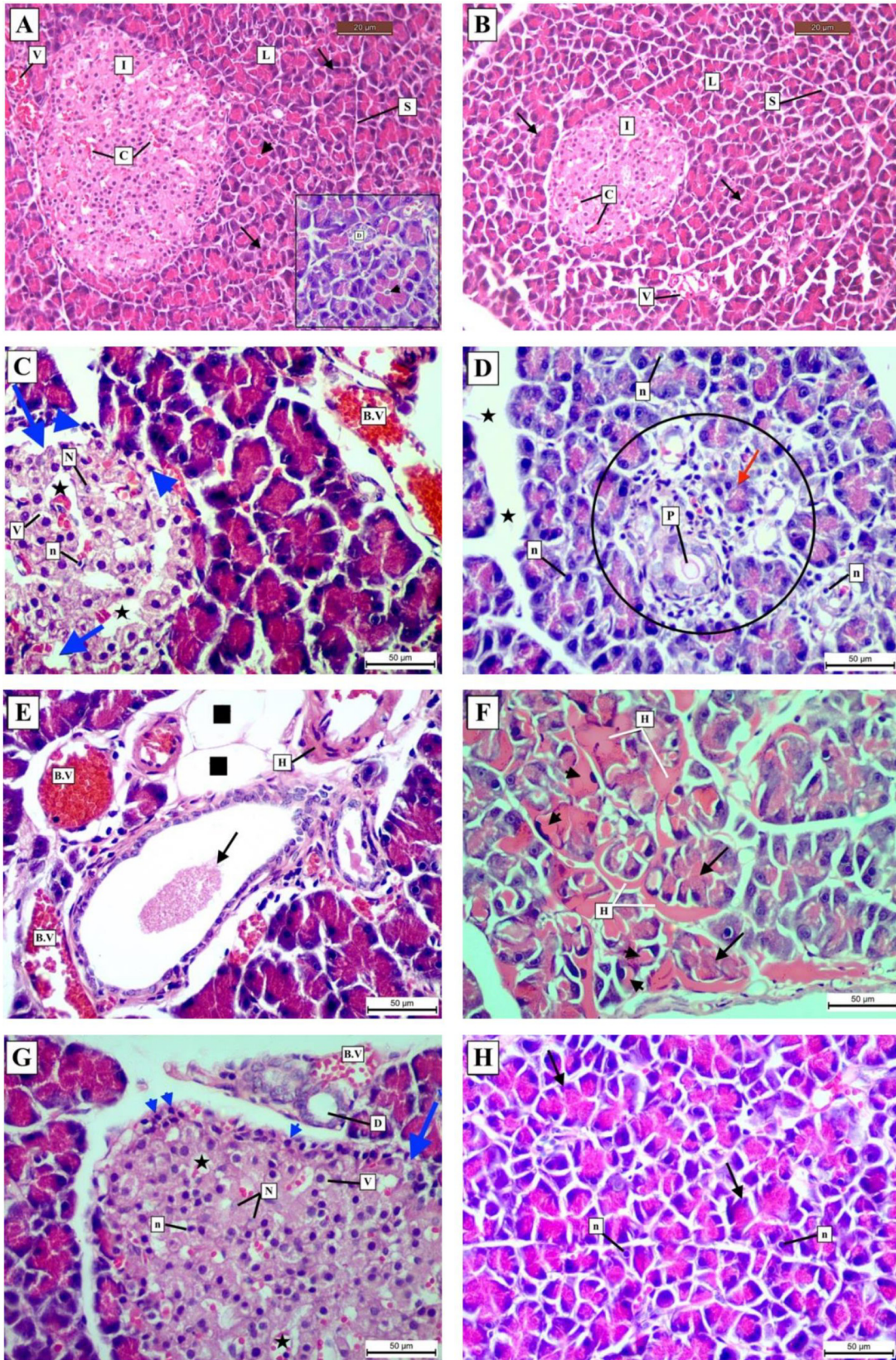
HFDQ group showed some islets with irregular outlines and less degenerated cells. The islet cells' mass was relatively decreased with moderately dilated blood sinusoids. Some islet cells showed cytoplasmic vacuoles. Few pyknotic and karyolitic nuclei and some

Table 1
Initial body weights, final body weights, relative pancreas and kidney weights in all studied groups in grams as mean ± standard deviation.

Groups	Initial body weight,	Final body weight	Relative pancreas weights	Relative kidney weights
Control	173.68 ± 12.65	230.78 ± 12.50	0.19720 ± 0.002	0.669 ± 0.0065
QE	172.45 ± 11.32	231.63 ± 13.13	0.19589 ± 0.003	0.668 ± 0.0063
HFD	175.67 ± 11.00	296.35 ± 13.60	0.20115 ± 0.004	0.671 ± 0.0055
HFDQ	176.79 ± 12.50	230.43 ± 13.00	0.19791 ± 0.002	0.670 ± 0.0054
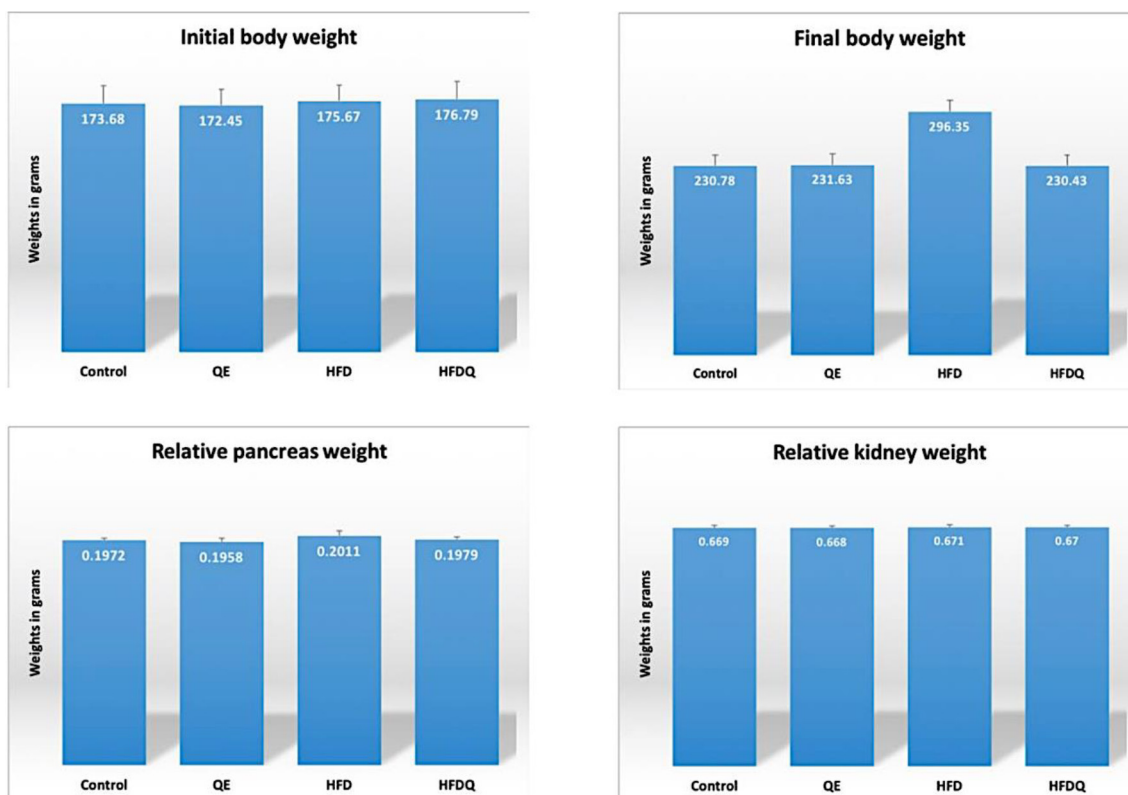
Histogram 1. Initial body weights, final body weights, relative pancreas and kidney weights in all studied groups in grams.

Rabab Ahmed Rasheed, M.S. Elshikh, Mohamed Othman Mohamed et al.

Journal of King Saud University – Science 34 (2022) 101946

Rabab Ahmed Rasheed, M.S. Elshikh, Mohamed Othman Mohamed et al.

Journal of King Saud University – Science 34 (2022) 101946

inflammatory cells were spotted as well. The blood vessels were less congested. Interlobular ducts had nearly normal caliber with a void lumen. The acini showed apparently normal histology like that of the control group except for a few pyknotic nuclei (Fig. 1 G&H) .

3.2.2. Renal tissue examination

Sections from control and QE group showed renal malpighian bodies were composed of a tuft of glomerular capillaries surrounded by a double-walled Bowman's capsule. The proximal convoluted tubules [PCT] had narrow lumina and high cuboidal deeply acidophilic epithelial cell lining with muffled boundaries and distinct brush border. The nuclei were round and vesicular. The distal convoluted tubules [DCT] were less numerous with wider lumina and lined with cubical less acidophilic epithelial cells (Fig. 4 A&B respectively).

HFD group showed several glomerular, tubular and interstitial lesions. Glomerular affection was presented as markedly reduced number of glomerular capillaries with dilated lumen, widened Bowman's space and shredded parietal layer. PCT lost their normal architecture. The tubular epithelial cells were severely degenerated with marked cytoplasmic vacuolization. Some tubules contained sloughed tubular cells in their lumina, forming granular casts with subsequent focally disrupted brush border. Large deposits of hyaline material were seen in tubular lumen. Nuclei of tubular cells showed pyknotic and karyolitic changes. (Fig. 4C). Interstitial tissue displayed mononuclear inflammatory cells, markedly congested blood vessel with extravasated RBCs and numerous recruited fibroblasts. Some vessels showed hyaline thickening of their walls. Interstitial areas of focal necrosis and rarefaction were also detected (Fig. 5 A,B&C). HFDQ group showed that the glomerular capillaries had apparently normal histology with standard number like those of the control group. Bowman's capsule showed average space with unvarying parietal layer. PCT were lined by relatively regular epithelium; however, some tubular epithelial cells were degenerated with cytoplasmic vacuolization. Sloughed tubular cells were seen in the lumen of some tubules with interrupted brush borders in some points. Few karyolitic nuclei were spotted. Interstitial tissue revealed mild to moderately congested vessels with some extravasated RBCs and few fibroblasts. Some vessels showed mild hyaline thickening of their walls (Fig. 4D&5D).

3.3. Morphometric results

The area percent of collagen fibers deposition in Mallory's trichrome stained sections and Bcl-2 expression in immunostained sections are presented as mean ± standard deviation in Table 2.

3.4. Statistical analysis

The statistical analysis of the morphometric results in both pancreatic and renal tissues revealed that there was no satistical significant difference between control and QE groups in all measured parameters. HFD group showed a highly significant increase ($p < 0.001$) in collagen fibers depositions as compared to all other groups, and a highly significant decrease ($p < 0.001$) in Bcl-2 expression as positive cytoplasmic reaction as compared to all other groups. While HFDQ group in both tissues showed a highly significant decrease ($p < 0.001$) in collagen fibers deposition and a highly significant increase ($p < 0.001$) in cytoplasmic Bcl-2 expression ($p < 0.001$) as compared to HFD group (Table 2) (Figs. 2,3,6 & 7).

4. Discussion

Excessive dietary intake of fat has long been linked to obesity which has currently assumed alarming proportions as a global public health concern. Chronic obesity and the accompanying deposition of fat in the tissues lead to a range of metabolic disorders, in particular, insulin resistance (IR) and type-2 diabetes mellitus. A link between HFD and oxidative stress (OS) has been recognized for a long (Vijayakumar et al., 2004). In the pancreas, the present histologic study revealed that HFD group showed various islet and acinar lesions. The islets appeared shredded with irregular contour. The islet cell mass was noticeably reduced. Many islet cells were disrupted and degenerated with markedly vacuolated cytoplasm. Many pyknotic and karyolitic nuclei were spotted as well. The blood sinusoids showed significant dilatation, and blood vessels were congested. This is in line with a previous work that stated that HFD-fed-rats showed diffuse areas of damage to both the endocrine and exocrine portions. Each islet itself had reduced number of cells besides, some rats showed a total absence of islets in the pancreas (Chung et al., 2018). According to (Barrientos et al., 2021) HFD has adverse effects on pancreatic β-cells denoted by increased pancreatic nuclear pyknosis and vacuolization, with fatty infiltration and structural alteration of the islets of Langerhans. This is maybe due to massive increase in cytosolic calcium accumulation, which may lead to rapid destruction of cells. β-cells changes may be due to the formation of reactive oxygen species (ROS). β-cells are specifically sensitive to oxidative stress because of their low levels of antioxidant enzyme (Abdul-Hamid and Moustafa, 2013). On the other hand, previous studies showed that the islet of Langerhans hyperplasia is associated with an augmented insulin level due to the development of insulin-resistance in HFD-treated mice model (Terauchi et al., 2007).

Fig. 1. Hx + E stained sections from pancreas of all studied groups: [A & B] control and QE respectively, showing typical pancreatic lobules (L) alienated by delicate interlobular septa (S) containing blood vessels (V). Lobules are formed of crowded acini (arrows) lined by pyramidal cells with basal vesicular nuclei, apical acidophilic zymogen granules and basal basophilic cytoplasm. Normally looking pale scattered islets of Langerhans (I) composed of clusters of hormone secreting cells with intervening fenestrated capillaries (C) are seen in between the islet cells. [X 200]. Notice: (Inset X 400) Centroacinose cell in the centre of acini (arrowhead) and intralobular duct (D) lined by simple cubical epithelium inside the lobule. [C] HFD group showing shredded islets with irregular contour (arrows), reduced islet cells' mass with vacuolated cytoplasm (V), pyknotic (n) and karyolitic (N) nuclei. Many cells are disrupted and degenerated (arrowheads). The islets' blood sinusoids are significantly dilated and congested (stars). The blood vessels are congested (B.V). [D] HFD group showing inflammatory cellular infiltrates invading the pancreatic lobules around the ducts and blood vessels (circle), many distorted acini with reparative attempts (arrow), inspissated plug (P) in intralobular duct, many pyknotic nuclei (n), and widened interlobular septa (stars). [E] HFD group showing markedly dilated interlobular duct with retained secretions (arrow), markedly congested (B.V) having thickened wall with eosinophilic hyaline material (H), and fatty infiltration adjacent to blood vessels (squares). [F] HFD group showing large deposits of intracellular hyaline material (arrowheads) and in between the acini (H). Many biased acini with fading of the basal cytoplasmic basophilia of acinar cells can be seen (arrows). [G] HFDQ group showing an islet with irregular outline (arrow) with less degenerated cells, relatively decreased islet cells' mass with moderately dilated blood sinusoids (stars), some islet cells show empty cytoplasmic fat vacuoles (V). Few pyknotic (n), karyolitic nuclei (N), and some inflammatory cells (arrowheads) are spotted. The blood vessels are less congested (B.V). Interlobular ducts have nearly normal caliber with void lumen (D). [H] HFDQ group showing apparently normal histology of pancreatic acini like that of the control group (arrows) except for few pyknotic nuclei (n). [X 400].
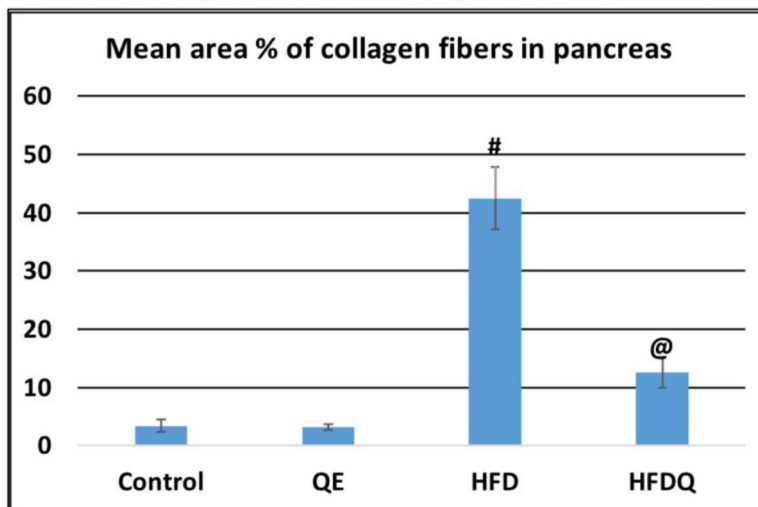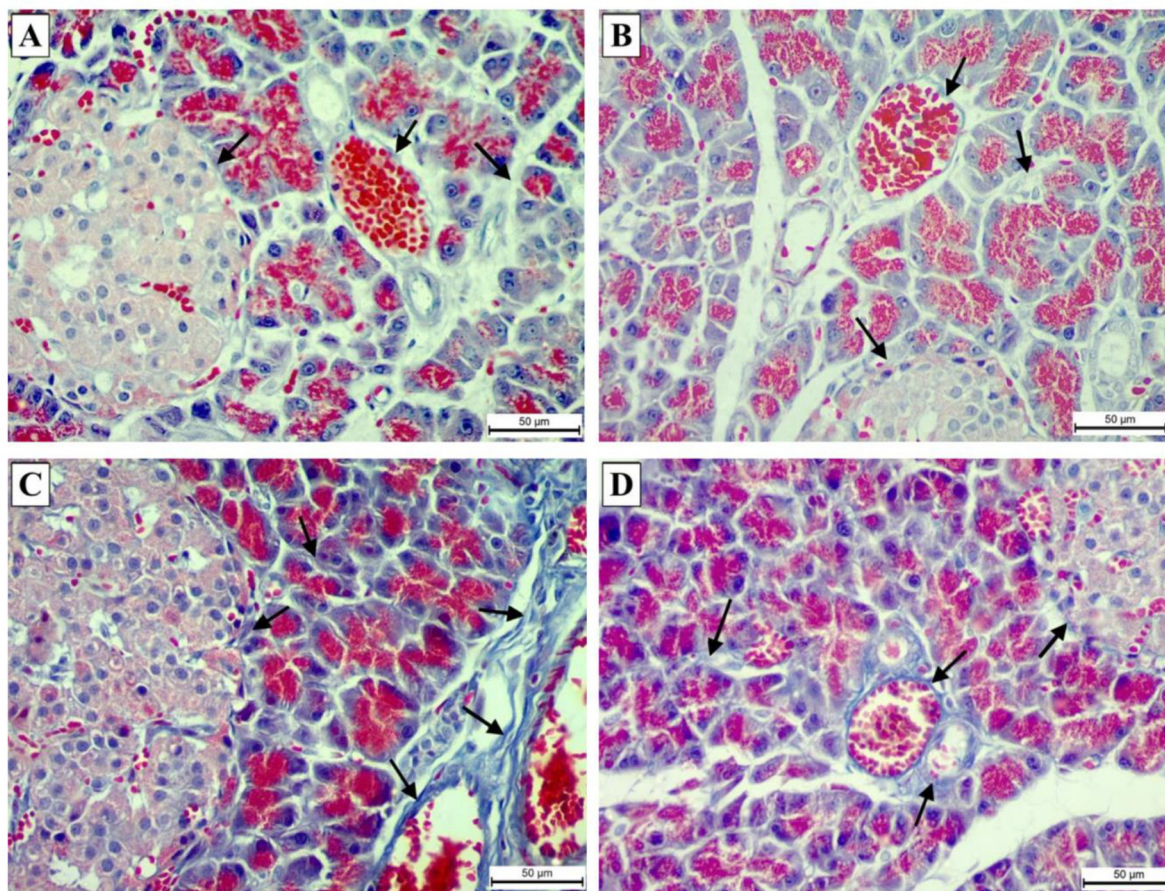
Rabab Ahmed Rasheed, M.S. Elshikh, Mohamed Othman Mohamed et al.

Journal of King Saud University – Science 34 (2022) 101946

Fig. 2. Mallory's trichrome stained sections from pancreas representing the amount of deposited collagen fibers in all studied groups: [A & B] Control and QE groups respectively, showing subtle blue collagen fibers (arrows). [C] HFD group displaying statistically highly significant increase in collagen fibers deposition (p < 0.001) as compared to HFDQ group presented as dense wavy collagen fibers around blood vessels and in between acini (arrows). [D] HFDQ group showing highly significant decrease in collagen fibers deposition (p < 0.001) as compared to HFD group presented as slight amount of collagen fibers (arrows). # highly significant to all groups, @ highly significant to HFD group [X 400].

HFD group in our research showed widened interlobular septa, markedly congested blood vessels whose walls were thickened with eosinophilic hyaline material. Moreover, large deposits of hyaline material could be obviously seen intracellular and in between the acini. Fatty infiltration could also be seen adjacent to ducts and blood vessels, this can be diagnosed as fat necrosis.

The key features of fat necrosis are the presence of many fat cells accompanied by inflammatory infiltrates and congested blood vessels (Bland et al., 2018). Fat necrosis confirms acute pancreatitis as harmonizes with (Dawra et al., 2007), who explained that by releasing lipases from necrotic pancreatic acinar cells. The present work demonstrated heavy inflammatory cellular infiltrates
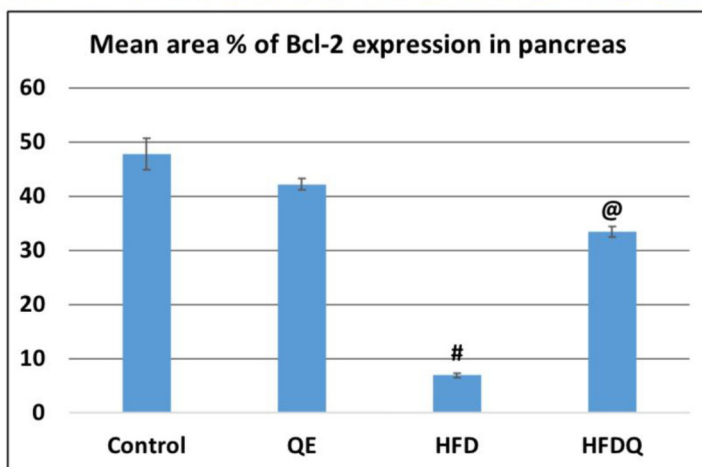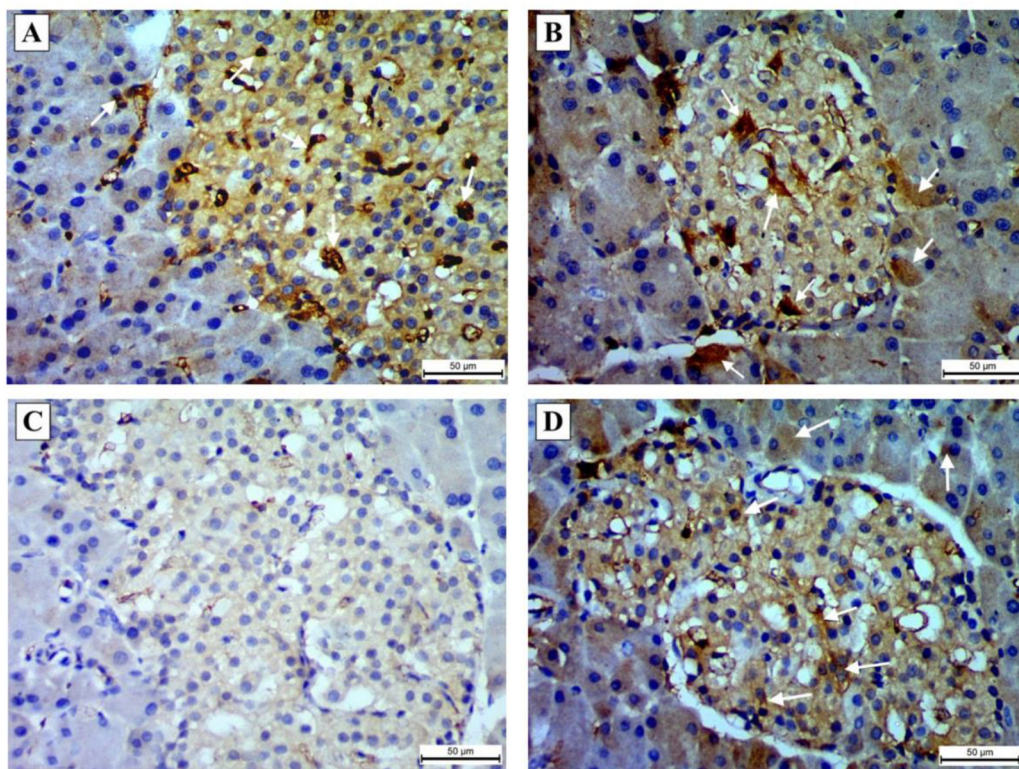
Rabab Ahmed Rasheed, M.S. Elshikh, Mohamed Othman Mohamed et al.

Journal of King Saud University – Science 34 (2022) 101946

Fig. 3. Immune-stained sections representing the Bcl-2 expression in the cytoplasm of islet and acinar pancreatic cells in all studied groups: [A & B] control and QE group respectively, showing positive cytoplasmic Bcl-2 expression (arrows). [C] HFD group displaying statistically highly significant decrease (p < 0.001) in Bcl-2 expression with negative reaction as compared to all other groups. [D] HFDQ group showing highly significant increase (p < 0.001) in Bcl-2 expression presented as positive cytoplasmic reaction as compared to HFD group (arrows). # highly significant to all groups, @ highly significant to HFD group [X 400].

invaded the pancreatic lobules and distorted many acini that showed reparative attempts. Several pyknotic nuclei were spotted. The interlobular ducts were dilated and contained retained secretions in their lumina. This agrees with previous work recruited that HFD aggravated the severity of acute pancreatitis (AP), as indicated by intense infiltration of immune cells and marked acinar cells necrosis. HFD could markedly exacerbate pancreatic oxidative stress and inflammatory response and lead to a more notable necroptosis during AP (Hong et al., 2020).

Histological findings of HFDQ group revealed a nearly normal pancreatic architecture. However, some islets showed irregular outlines with less degenerated cells. The islet cells' mass was relatively decreased with moderately dilated blood sinusoids. Some islet cells showed empty cytoplasmic vacuoles, few pyknotic and karyolitic nuclei. Some inflammatory cells and less congested vessels were seen. Interlobular ducts had nearly normal caliber with void lumen. The acini showed apparently normal histology like that of the control group except for a few pyknotic nuclei. This
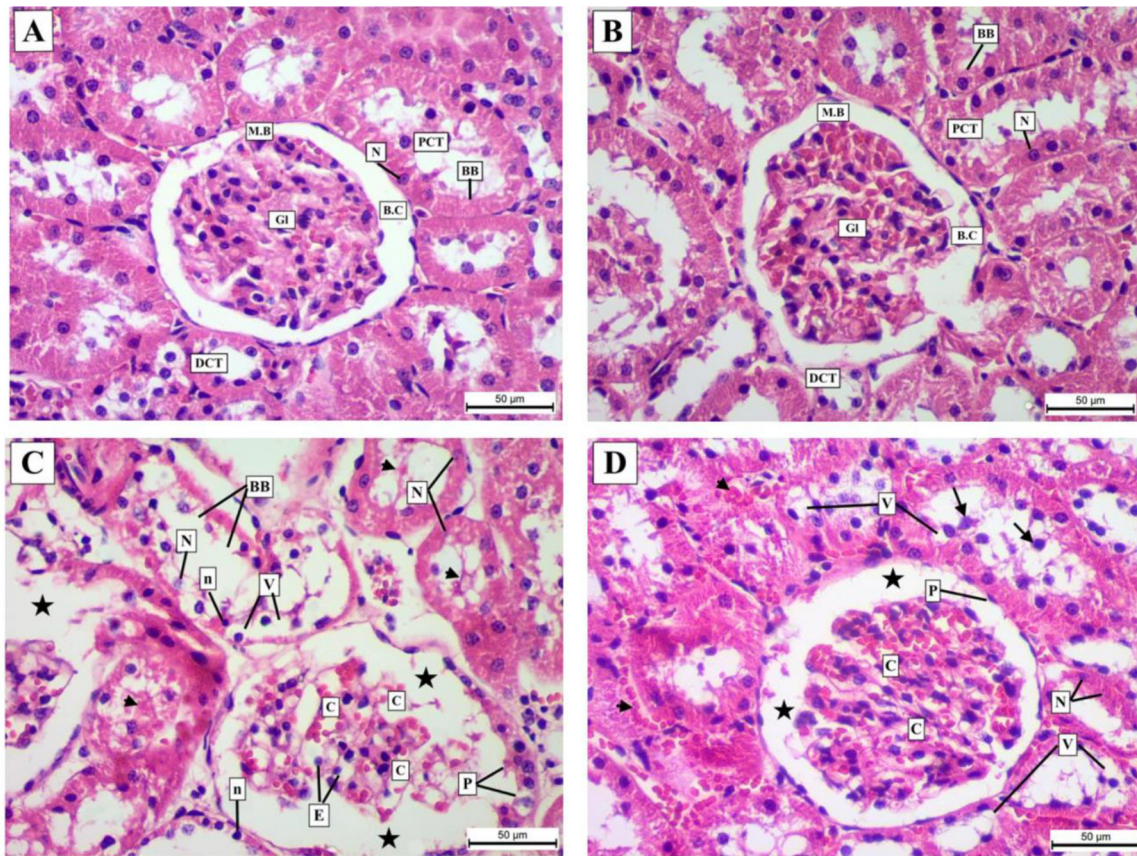
Rabab Ahmed Rasheed, M.S. Elshikh, Mohamed Othman Mohamed et al.

Journal of King Saud University – Science 34 (2022) 101946

Fig. 4. Hx + E stained sections from kidney: [A & B] control and QE groups respectively showing malpighian bodies (M.B) composed of a tuft of glomerular capillaries (Gl) surrounded by a double-walled Bowman's capsule (B.C). The proximal convoluted tubules (PCT) are plentiful with narrow lumina and high cuboidal deeply acidophilic epithelial cell lining with muffled boundaries and distinct brush border (BB). The nuclei are round and vesicular (N). The distal convoluted tubules (DCT) are less numerous with wider lumina, lined with cubical less acidophilic epithelial cells. [C] HFD group showing markedly reduced number of glomerular capillaries with dilated lumen (C) and plump endothelial lining (E), widened Bowman's capsule (stars) and shredded parietal layer (P). PCT lost their normal architecture with severely degenerated epithelial cell lining and marked cytoplasmic vacuolization (V). Tubular lumina show sloughed epithelial cells forming granular casts (arrowheads). The brush border of tubular cells is focally disrupted (BB). Many nuclei show pyknotic (n) and karyolitic (N) changes. [D] HFDQ group showing apparently normal histology of glomerular capillaries with standard number like those of the control group (C), average Bowman's space (stars) with unvarying parietal layer (P), vacuolated tubular cells (V), sloughed tubular cells in lumen (arrows), few karyolitic nuclei (N), and extravasated RBCs in interstitial tissue (arrowheads) [X 400].

improvement could indicate the powerful antioxidant effect of QE, which can prevent oxidative stress and delay the progression of HFD complications by suppressing the release of inflammatory factors (chemokines and cytokines) (Shi et al., 2019). Also, improving mitochondrial bioenergetic function and stimulating amplifying pathways of insulin secretion are likely the main mechanisms by which flavonoids preserve the secretory capacity of β-cells as stated by (Ghorbani et al., 2019).

The kidney is an organ highly vulnerable to damage caused by ROS, likely due to the abundance of polyunsaturated fatty acids in the composition of renal lipids. ROS are involved in the pathogenic mechanism of conditions such as glomerulosclerosis and tubulointerstitial fibrosis (Khaksary-Mahabady et al., 2018). In the current study, sections from rats of HFD group showed markedly reduced number of glomerular capillaries with dilated lumen, widened Bowman's space with shredded parietal cell layer, markedly congested blood vessels with extravasated RBCs and marked mononuclear inflammatory infiltrates in interstitial tissue. Some vessels showed hyaline thickening of their walls. Rarefaction, necrosis, and numerous recruited fibroblasts were spotted in focal areas within renal interstitial tissues as well. These results are in accordance with another study which showed dilatation in glomerular capillaries and mononuclear cell infiltration, degeneration in nephrons marked by glomerulosclerosis, segmental necro-

sis, tubular defects and many necrotic interstitial cells (Salim et al., 2018). The present work revealed that PCT lost their normal architecture, the lining epithelial cells were severely degenerated with marked cytoplasmic vacuolization. Some cells were sloughed inside PCT's lumen, and the brush border was disrupted. Many nuclei showed pyknotic and karyolitic changes. The lumina of many PCT were occupied by granular casts and large deposits of hyaline material. Some tubules had dilated lumen and were lined by low cubical to flat epithelium.

These findings are in line with (Bin-Meferij et al., 2019; Tanaka et al., 2009) who stated that PCT of HFD-treated rats showed irregular pyknotic nuclei of their lining epithelium with their brush margin was destructed. Also, the cytoplasm contained numerous vacuoles, lysosomes, mitochondria with electron-lucent matrix a large number of cytosomes and lipid droplets. On the other hand, another work recruited an increased number of glomerular cells in the kidney of HFD group. Also, the glomerular mesangial matrix increased, and obvious epithelial proliferation of kidney tubules was observed (Zhang et al., 2016).

The present study revealed that sections from rats of HFDQ group showed that the glomerular capillaries had apparently normal histology with standard numbers like those of the control group with average Bowman's space and unvarying parietal layer. PCT were lined by relatively regular epithelium. However, some
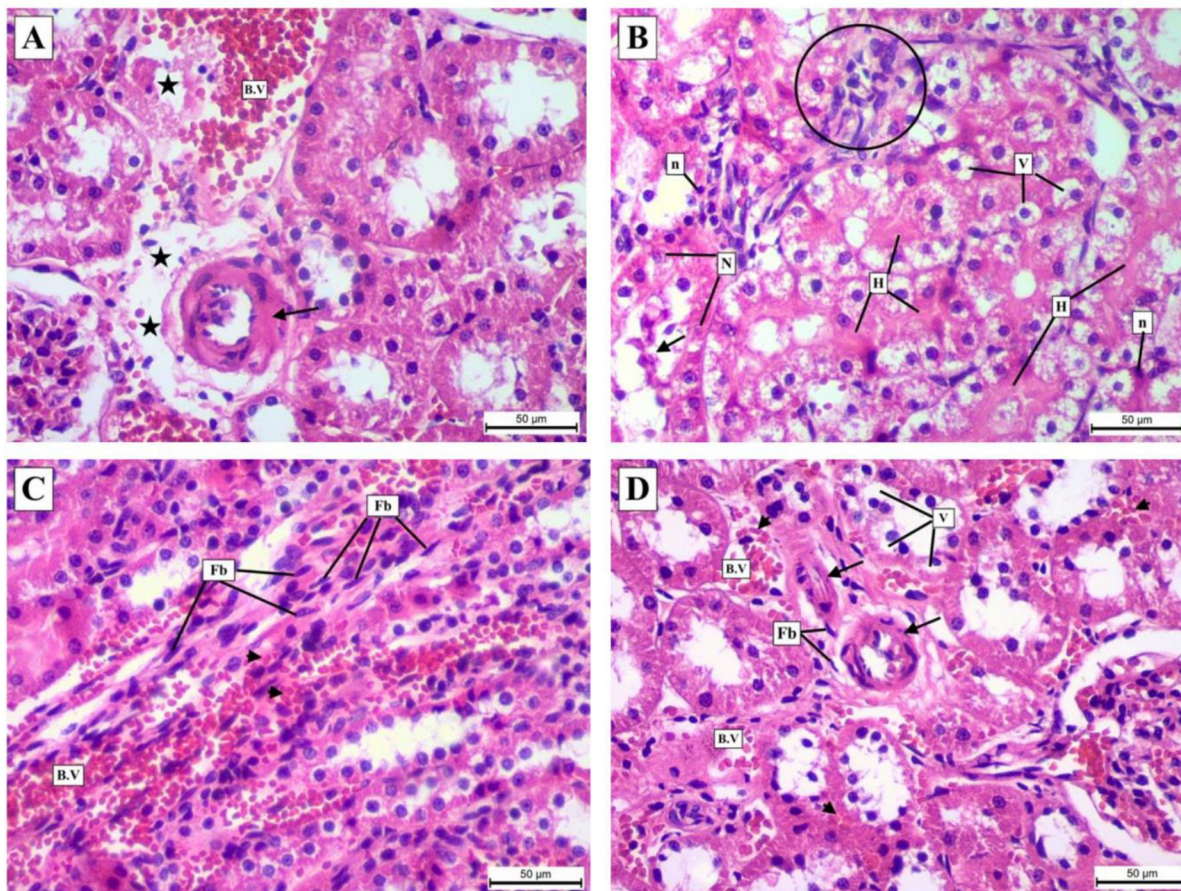
Fig. 5. Hx + E stained sections of renal tissue from rats of HFD and HFDQ groups: [A] HFD group showing markedly congested blood vessels (B.V), hyaline thickening of vessels' wall (arrow), and focal interstitial rarefaction and necrosis (stars). [B] HFD group showing disorganized PCTs lined by severely degenerated epithelium with markedly vacuolated cytoplasm (V), sloughed epithelial cells in tubular lumen (arrow), pyknotic (n) and karyolitic (N) nuclei. The tubular lumen is obliterated by large deposits of hyaline material (H). Mononuclear inflammatory cells are spotted (circle). [C] HFD group showing congested vessels (B.V), marked extravasated RBCs (arrowheads), and vast number of recruited fibroblasts (Fb). [D] HFDQ group showing vacuolated tubular cells (V), moderately congested vessels (B.V), interstitial extravasated RBCs (arrowheads), and few fibroblasts (Fb). [X 400].

Table 2
Comparison between different studied groups in pancreas and kidney according to mean area % of collagen fibers and Bcl-2 expression ± Standard Deviation.

	Collagen fibers [Mean area % ± SD]		Bcl-2 expression [Mean area % ± SD]	
	Pancreas	Kidney	Pancreas	Kidney
Control	3.4 ± 1.1	3.9 ± 1.3	47.8 ± 2.9	48.9 ± 9.6
QE	3.2 ± 0.5	4.2 ± 0.7	42.2 ± 1.0	49.6 ± 6.6
HFD	42.5 ± 5.3[#]	42.4 ± 0.8[#]	6.9 ± 0.4[#]	7.5 ± 1.8[#]
HFDQ	12.6 ± 2.7[@]	11.7 ± 0.7[@]	33.4 ± 0.9[@]	35.7 ± 4.4[@]

SD: Standard deviation.
[#] Highly significant (P < 0.001) as compared to all studied groups.
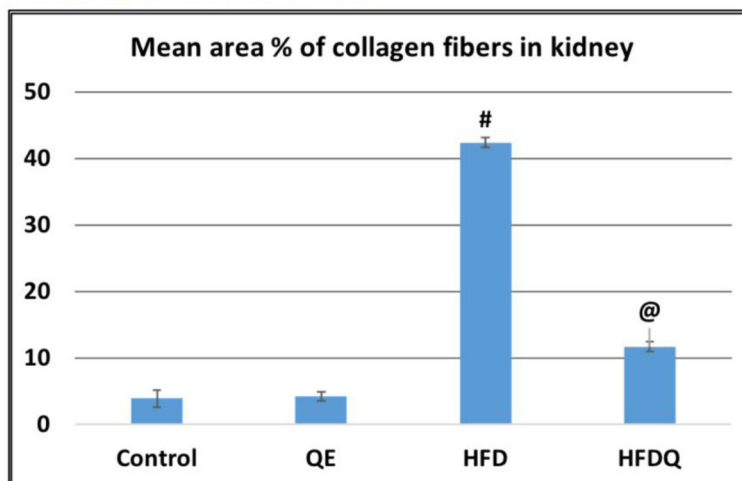[@] Highly significant (P < 0.001) as compared to HFD group.

Rabab Ahmed Rasheed, M.S. Elshikh, Mohamed Othman Mohamed et al.

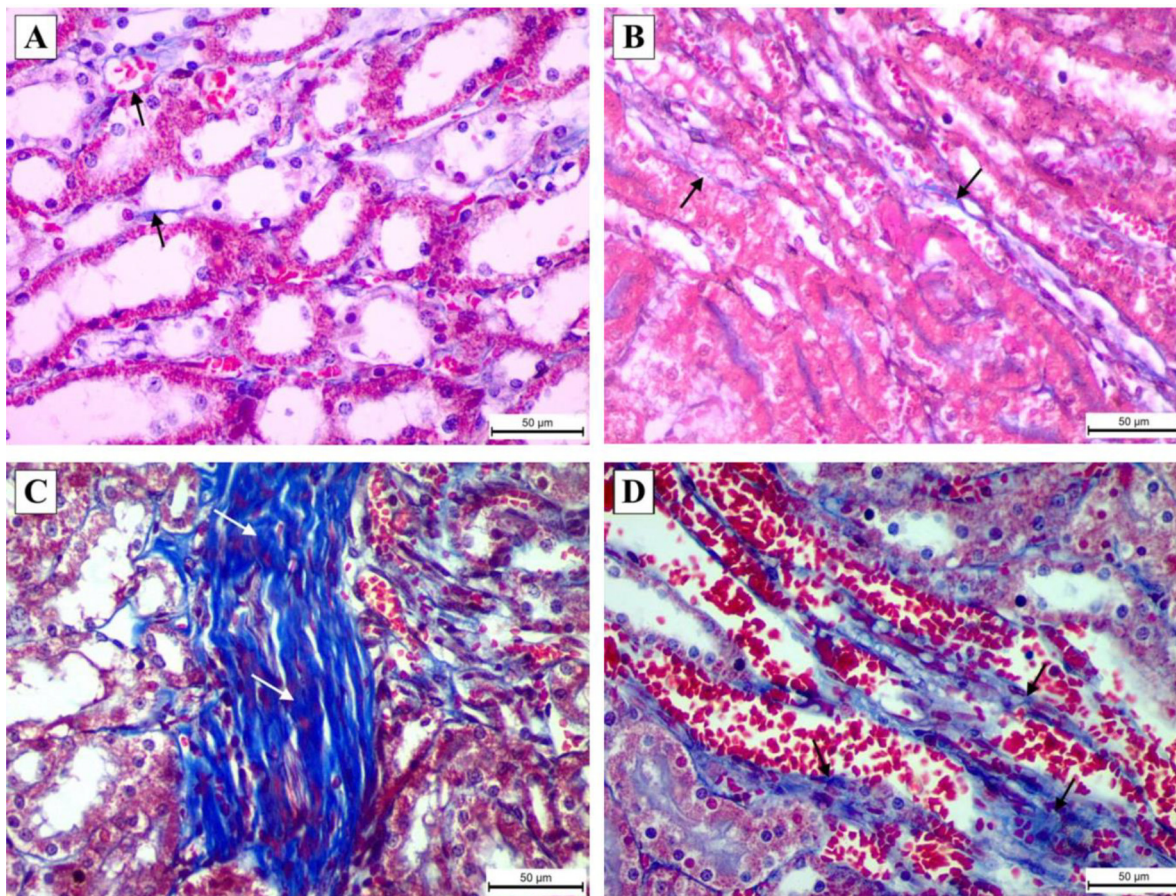*Journal of King Saud University – Science 34 (2022) 101946*

Fig. 6. Mallory's trichrome stained sections from kidney representing the amount of deposited collagen fibers in all studied groups: [A & B] control and QE group respectively, showing delicate blue collagen fibers in renal tissue (arrows). [C] HFD group displaying a statistically highly significant increase (p < 0.001) in collagen shown as dense interstitial wavy bundles as compared to all other groups (arrows). [D] HFDQ group showing highly significant decrease in collagen depositions (p < 0.001) shown as little collagen fibers as compared to HFD group [arrows]. # highly significant to all groups, @ highly significant to HFD group [X 400].
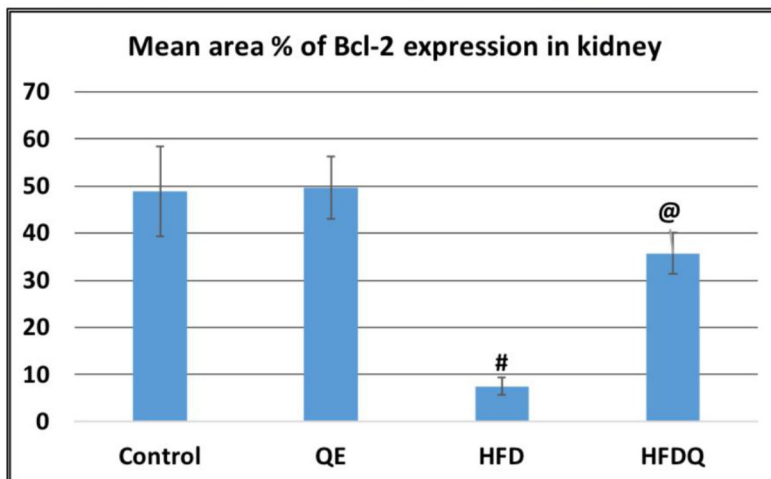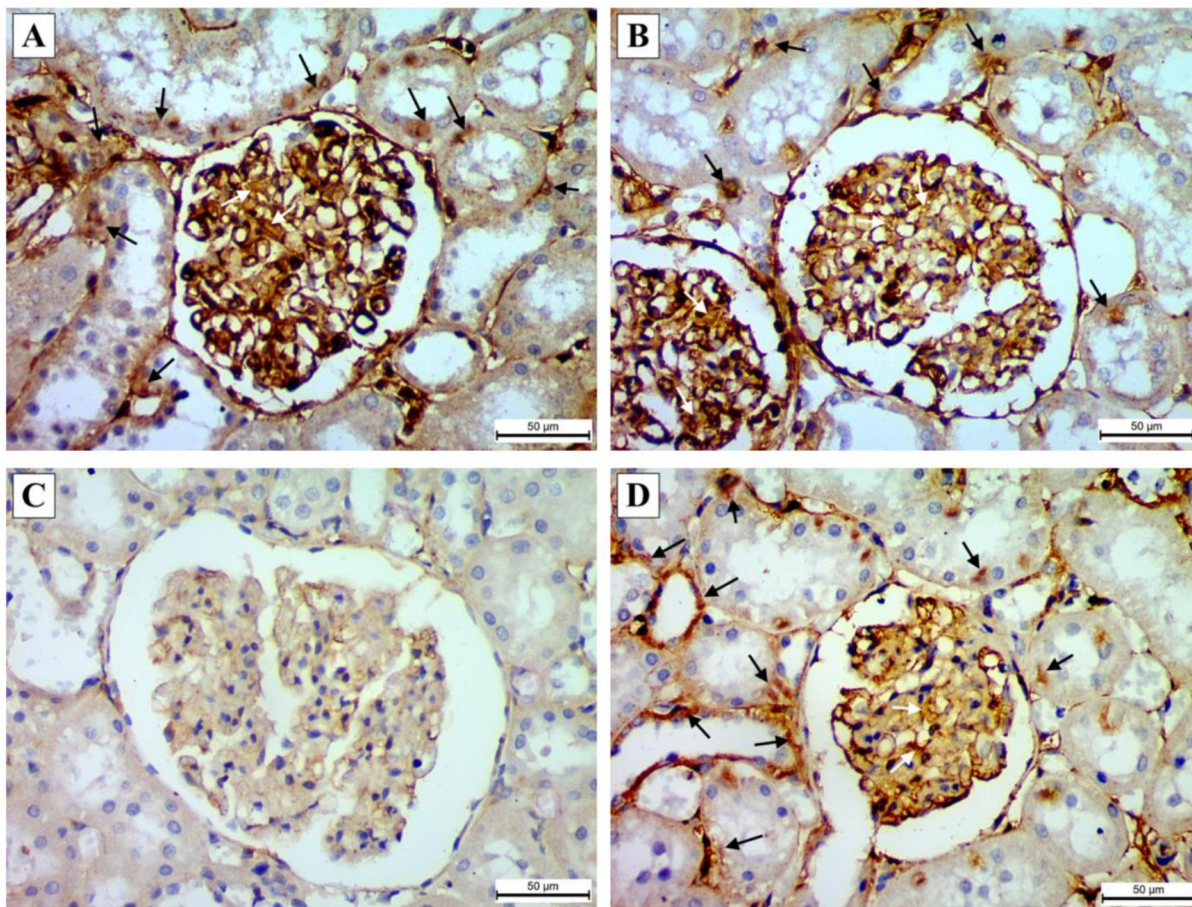
Rabab Ahmed Rasheed, M.S. Elshikh, Mohamed Othman Mohamed et al.

Journal of King Saud University – Science 34 (2022) 101946

Fig. 7. Immune-stained sections representing Bcl-2 expression in the cytoplasm of glomerular and tubular renal cells in all studied groups: [A & B] control and QE groups respectively, showing positive Bcl-2 expression in the cytoplasm of glomerular and tubular cells (arrows). [C] HFD group showing a highly significant decrease in Bcl-2 expression (p < 0.001) as compared to all other groups. [D] HFDQ group showing a highly statistically significant increase (p < 0.001) Bcl-2 expression presented as positive reaction as compared to HFD group (arrows). # highly significant to all groups, @ highly significant to HFD group [X 400].

tubular epithelial cells were degenerated with cytoplasmic vacuolization. Sloughed epithelial cells and masses of hyaline material were encountered in the lumina of some tubules. The brush border was interrupted in some areas. Few karyolitic nuclei were spotted. The blood vessels showed mild to moderate congestion with some extravasated RBCs in between the tubules. Other vessels revealed mild hyaline thickening of their walls. Few fibroblasts were detected in the renal interstitium.

According to (Al-Rasheed et al. 2013) QE could scavenge free radicals and inhibit xanthine oxidase and lipid peroxidation. It protects against oxidative damage in renal tubular cells and renal tissues. A previous study ascertained that the histological analysis of the renal cortex of QE treated group showed that the tubular cells, glomerular parts, and interstitial tissue had normal morphology. The administration of QE improved the tubular structure where damage to the tubular cells was not observed, and the glomeruli appeared normal with capsular space (Sedky et al., 2017). (Liu et al., 2010) stated that QE could protect the rat kidney against lead induced injury by improving renal function, attenuating histopathologic changes, reducing ROS production, renewing the activities of antioxidant enzymes, decreasing DNA oxidative damage and apoptosis. Mallory's trichrome stained sections of both pancreatic and renal tissues showed minimal collagen fibers deposition in groups Control and QE group while, HFD group displayed dense wavy collagen fibers around blood vessels and in interstitial tissues. Sections from HFDQ group showed little collagen deposition. The mean area% of collagen fibers showed a highly significant increase in HFD group as compared to all other groups. On the other hand, it showed a highly significant decrease in HFDQ group as compared to HFD group.

This could be explained by activation of pancreatic stellate cells by oxidative stress or releasing inflammatory cytokines like interleukin-1, interleukin-6 and transforming growth factors. They differentiate to fibroblast like cells forming collagen types I, II and fibronectin (Abd El-Haleem and Mohamed, 2012). This is in harmony with (Marcolin et al., 2012) who stated that treatment with QE exerts an antifibrogenic action at multiple levels depending mainly on the modulation of the profibrogenic signals generated by inflammation and oxidative stress. Alongside, results obtained from a prior study demonstrated that HFD developed renal injury with increased inflammatory cytokine expression that resembled the characteristics of CKD. It is plausible that the development of renal fibrosis may become apparent after a longer period of HFD feeding (Madduma et al., 2020). In the same context, it was revealed that QE administration showed anti-renal fibrotic effects in vitro and in vivo through inhibition of renal injury, inflammatory cell infiltration and fibrogenesis. Moreover, QE also showed its protective effects by inhibition of excessive extracellular matrix (ECM) accumulation (Liu et al., 2019). Immunostained sections of both pancreatic and renal tissues showed marked a positive Bcl-2 expression in groups Control and QE in the cytoplasm, while HFD group displayed negative Bcl-2 expression. HFDQ Group exhibited positive Bcl-2 expression. About the mean area% of Bcl-2 expression, it showed a highly significant decrease in HFD group as compared to all other groups and a highly significant increase in HFDQ group versus HFD group. This agrees with a former work that stated that QE, in a dose-dependent manner, potentially attenuated the oxidative stress induced by D-gal in the pancreatic and renal tissues of rats through the upregulation of antioxidant, antiapoptotic (Bcl-2), and functional markers. Also, quercetin downregulated apoptotic (Bax and Casp-3), and inflammatory (TNF) markers (El-Far et al., 2020). Moreover, a recent study disclosed that HFD resulted in substantial changes in metabolic parameters, lipid profile, renal functional markers, oxidative stress, inflammatory and apoptosis markers in kidneys of diabetic rats (Guo et al.,

2021). Taking together, (Rasheed et al., 2021) ascertained that HFD-fed rats had an adverse effect on cardiomyocytes that showed atrophy and degenerative changes with vacuolated sarcoplasm and congested vasculature. Administration of quercetin to rats' diet has markedly improved the cardiomyocytes both histologically and ultra-structurally.

5. Conclusions

In recent years, QE has received widespread attention due to its exciting pharmacological potential and health benefits. In this study, we comprehensively summarized the histologic improvement in the pancreas and kidney in HFD fed-rats treated with QE. Besides, many clinical trials have proven the impact of QE treatment on patients with diabetes, hyperlipidemia, and NAFLD. In this respect, additional researches are necessary to further evaluate the dose–response protective effect of QE on systemic organs in these three diseases. The completion of these studies is expected to provide a scientific basis for the therapeutic potential of QE in human subjects.

Declaration of Competing Interest

The authors declare that they have no known competing financial interests or personal relationships that could have appeared to influence the work reported in this paper.

Appendix A. Supplementary data

Supplementary data to this article can be found online at https://doi.org/10.1016/j.jksus.2022.101946.

References

Abd El-Haleem, M.R., Mohamed, D.A., 2012. The effects of experimental aflatoxicosis on the pancreas of adult male albino rats and the role of ginger supplementation: a histological and biochemical study. Egypt. J. Histol 34, 423–435. https://doi.org/10.1097/EHX.0000398847.67845.55.

Abdul-Hamid, M., Moustafa, N., 2013. Protective effect of curcumin on histopathology and ultrastructure of pancreas in the alloxan treated rats for induction of diabetes. J. Basic Appl. Zool. 66 (4), 169–179. https://doi.org/10.1016/j.jobaz.2013.07.003.

Al-Rasheed, N.M., Faddah, L.M., Mohamed, A.M., Abdel Baky, N.A., Al-Rasheed, N.M., Mohammad, R.A., 2013. Potential impact of quercetin and idebenone against immuno- inflammatory and oxidative renal damage induced in rats by titanium dioxide nanoparticles toxicity. J. Oleo Sci. 62 (11), 961–971. https://doi.org/10.5650/jos.62.961.

Barrientos, C., Pérez, A., Vázquez, J., 2021. Ameliorative effects of oral glucosamine on insulin resistance and pancreatic tissue damage in experimental wistar rats on a high-fat diet. Comp Med. 71 (3), 215–221. https://doi.org/10.30802/AALAS-CM-21-000009.

Bin-Meferij, M.M., El-Kott, A.F., Shati, A.A., Eid, R., 2019. Ginger extract ameliorates renal damage in high fat diet-induced obesity in rats: biochemical and ultrastructural study. Int. J. Morphol. 37 (2), 438–447. https://doi.org/10.4067/S0717-95022019000200438.

Bland, K.I., Copeland, E.M., Klimberg V.S., Gradishar, W.J., 2018. The Breast: Comprehensive Management of Benign and Malignant Diseases. Fifth ed., Elsevier. Philadelphia. 13: 177–196. https://doi.org/10.1016/C2014-0-01946-6.

Cao, Y., Bao, S., Yang, W., Zhang, J., Li, L., Shan, Z., Teng, W., 2014. Epigallocatechin gallate prevents inflammation by reducing macrophage infiltration and inhibiting tumor necrosis factor-α signaling in the pancreas of rats on a high-fat diet. Nutr. Res. 34 (12), 1066–1074.

Chung, A., Gurtu, S., Chakravarthi, S., Moorthy, M., Palanisamy, U.D., 2018. Geraniin protects high-fat diet-induced oxidative stress in sprague dawley rats. Front Nutr. 5, 17. https://doi.org/10.3389/fnut.2018.00017.

Rabab Ahmed Rasheed, M.S. Elshikh, Mohamed Othman Mohamed et al.

Journal of King Saud University – Science 34 (2022) 101946

Dawra, R., Sharif, R., Phillips, P., Dudeja, V., Dhaulakhandi, D., Saluja, A.K., 2007. Development of a new mouse model of acute pancreatitis induced by administration of L-arginine. Am J Physiol Gastrointest Liver Physiol 292, G1009–G1018. https://doi.org/10.1152/ajpgi.00167.2006.

Dominguez, J.H., Tang, N., Xu, W., Evan, A.P., Siakotos, A.N., Agarwal, R., Walsh, J., Deeg, M., Pratt, J.H., March, K.L., Monnier, V.M., Weiss, M.F., Baynes, J.W., Peterson, R., 2000. Studies of renal injury III: lipid-induced nephropathy in type II diabetes. Kidney Int. 57 (1), 92–104. https://doi.org/10.1046/j.1523-1755.2000.00814.x.

Ekeleme-Egedigwe, C.A., Ijeh, I.I., Okafor, P.N., 2017. Modulatory effects of dietary supplementation by Vernonia amygdalina on high-fat-diet-induced obesity in Wistar rats. Acta Sci. Pol. Technol. Aliment. 16(4) 2017, 431–442. https://doi.org/10.17306/J.AFS.0504.

El-Far, A. H., Lebda, M. A., Noreldin, A. E., Atta, M. S., Elewa, Y., Elfeky, M., & Mousa, S. A. (2020). Quercetin attenuates pancreatic and renal D-galactose-induced aging-related oxidative alterations in rats. Int. J. Mol. Sci., 18; 21(12):4348. https://doi.org/10.3390/ijms21124348

Emsley, R., Dunn, G., White, I.R., 2010. Mediation and moderation of treatment effects in randomised controlled trials of complex interventions. Stat. Meth. Med. Res. 19 (3), 237–270. https://doi.org/10.1177/0962280209105014.

Ghorbani, A., Rashidi, R., Shafiee-Nick, R., 2019. Flavonoids for preserving pancreatic beta cell survival and function: a mechanistic review. Biomed. Pharmacother. 111, 947–957.

Guo, J., Li, J., Wei, H., Liang, Z., 2021. Maackiain protects the kidneys of type 2 diabetic rats via modulating the Nrf2/HO-1 and TLR4/NF-κB/caspase-3 pathways. Drug Des Devel Ther. 15, 4339–4358. https://doi.org/10.2147/DDDT.S326975.

Hong, Y.P., Yu, J., Su, Y.R., Mei, F.C., Li, M., Zhao, K.L., Zhao, L., Deng, W.H., Chen, C., Wang, W.X., 2020. High-fat diet aggravates acute pancreatitis via TLR4-mediated necroptosis and inflammation in rats. Oxid. Med. Cell. Longev. https://doi.org/10.1155/2020/8172714. 8172714.

Jarvis, S., Gethings, L.A., Samanta, L., Pedroni, S., Withers, D.J., Gray, N., Plumb, R.S., Winston, R., Williamson, C., Bevan, C.L., 2020. 2020, High fat diet causes distinct aberrations in the testicular proteome. Int. J. Obes. 44, 1958–1969. https://doi.org/10.1038/s41366-020-0595-6.

Ježek, P., Jabůrek, M., Plecitá-Hlavatá, L., 2019. Contribution of oxidative stress and impaired biogenesis of pancreatic β-cells to type 2 diabetes. Antioxid. Redox Signal. 31 (10), 722–751. https://doi.org/10.1089/ars.2018.7656.

Khaksary-Mahabady, M., Ranjbar, R., Najafzadeh-Varzi, H., Mohammadian, B., Gohari-Behbahani, N., 2018. Protective effect of quercetin on histomorphometric changes in kidney of retinoid acid-treated rat fetuses. Int. J. Morphol. 36 (1), 338–344. https://doi.org/10.4067/S0717950222018000100338.

Kiernan, J.A., 2015. Histological and histochemical methods; theory and practice. J. Anat., 238–310 https://doi.org/10.1111/joa.12390.

Ko, M.J., Mulia, G.E., van Rijn, R.M., 2019. Commonly used anesthesia/euthanasia methods for brain collection differentially impact MAPK activity in male and female C57BL/6 mice. Front. Cell. Neurosci. 13, 96. https://doi.org/10.3389/fncel.2019.00096.

Kovesdy, C.P., Furth, S., Zoccali, C., World Kidney Day Steering Committee, 2017. Obesity and kidney disease: hidden consequences of the epidemic. Physiol. Int. 104 (1), 1–14. https://doi.org/10.1556/2060.104.2017.1.9.

Liu, C.M., Ma, J.Q., Sun, Y.Z., 2010. Quercetin protects the rat kidney against oxidative stress-mediated DNA damage and apoptosis induced by lead. Environ. Toxicol. Pharmacol. 30 (3), 264–271. https://doi.org/10.1016/j.etap.2010.07.002.

Liu, X., Sun, N., Mo, N., Lu, S., Song, E., Ren, C., Li, Z., 2019. Quercetin inhibits kidney fibrosis and the epithelial to mesenchymal transition of the renal tubular system involving suppression of the Sonic Hedgehog signaling pathway. Food Funct. 10, 3782. https://doi.org/10.1039/c9fo00373h.

Marcolin, E., San-Miguel, B., Vallejo, D., Tieppo, J., Marroni, N., González-Gallego, J., Tuñón, M.J., 2012. Quercetin treatment ameliorates inflammation and fibrosis in mice with nonalcoholic steatohepatitis. J. Nutr. 142 (10), 1821–1828. https://doi.org/10.3945/jn.112.165274.

Madduma, H.S., Prashar, S., Debnath, S.C., Siow, Y.L., 2020. Inhibition of inflammatory cytokine expression prevents high-fat diet-induced kidney injury: role of lingonberry supplementation. Front. Med. (Lausanne). 7, 80. https://doi.org/10.3389/fmed.2020.00080.

Matuszewska, J., Ziarniak, K., Dudek, M., Kołodziejski, P., Pruszyńska-Oszmałek, E., Śliwowska, J.H., 2020. Effects of short-term exposure to high-fat diet on histology of male and female gonads in rats. Acta Histochem. 122, (5). https://doi.org/10.1016/j.acthis.2020.151558 151558.

Muñoz-García, B., Moreno, J.A., López-Franco, O., Sanz, A.B., Martín-Ventura, J.L., Blanco, J., Jakubowski, A., Burkly, L.C., Ortiz, A., Egido, J., Blanco-Colio, L.M., 2009. Tumor necrosis factor-like weak inducer of apoptosis (TWEAK) enhances vascular and renal damage induced by hyperlipidemic diet in ApoE-knockout mice. Arterioscler. Thromb. Vasc. Biol 29 (12), 2061–2068. https://doi.org/10.1161/ATVBAHA.109.194852.

Mzhelskaya, K.V., Trusov, N.V., Apryatin, S.A., Soto, C.J., Gmoshinski, I.V., Tutelyan, V. A., 2019. Effect of quercetin on the expression of the carbohydrate and lipid metabolism genes in the liver of rats with genetic. Vopr. Pitan. 88 (2), 6–16. https://doi.org/10.24411/0042-8833-2019-10012.

Mzhelskaya, K.V., Shipelin, V.A., Shumakova, A.A., Musaeva, A.D., Soto, J.S., Riger, N. A., Trusov, N.V., Kirbaeva, N.V., Apryatin, S.A., Gmoshinski, I.V., 2020. Effects of

quercetin on the neuromotor function and behavioral responses of Wistar and Zucker rats fed a high-fat and high-carbohydrate diet. Behav. Brain Res. 27, (378). https://doi.org/10.1016/j.bbr.2019.112270 112270.

Park, Y., Jang, I., Park, H.Y., Kim, J., Lim, K., 2020. Hypoxic exposure can improve blood glycemic control in high-fat diet-induced obese mice. Phys. Act. Nutr. 24 (1), 19–23. https://doi.org/10.20463/pan.2020.0004.

Perez-Vizcaino, F., Duarte, J., Jimenez, R., Santos-Buelga, C., Osuna, A., 2009. Antihypertensive effects of the flavonoid quercetin. Pharmacol. Rep. 61 (1), 67–75. https://doi.org/10.1016/s1734-1140(09)70008-8.

Ramos-Vara, J.A., Miller, M.A., 2014. When tissue antigens and antibodies get along: revisiting the technical aspects of immunohistochemistry–the red, brown, and blue technique. Vet. Pathol. 51 (1), 42–87. https://doi.org/10.1177/0300985813505879.

Rasheed, R., Othman, M., Hussein, U., Embaby, A., 2021. The possible ameliorative influence of quercetin on cardiac muscle changes induced by high fat diet in adult male albino rats: light and electron microscopic study. https://doi.org/10.21608/EJH.2021.76868.1484.

Salim, H.M., Kurnia, L.F., Bintarti, T.W., Handayani, H., 2018. The effects of high-fat diet on histological changes of kidneys in rats. Biomol. Health Sci. 1 (2), 109–112. https://doi.org/10.20473/bhsj.v1i2.9675.

Sedky, A., Mahboub, F., Elsawy, H., Eid, R., 2017. Protective potential of quercetin on Cd-induced hepatorenal damage. Pol. J. Environ. Stud. 26 (5). https://doi.org/10.15244/pjoes/68954.

Shaw, O.M., Harper, J.L., 2013. An efficient single prime protocol for the induction of antigen-induced airways inflammation. J. Immunol. Methods 395 (1), 79–82. https://doi.org/10.1016/j.jim.2013.06.007.

Shi, G.J., Li, Y., Cao, Q.H., Wu, H.X., Tang, X.Y., Gao, X.H., Yu, J.Q., Chen, Z., Yang, Y., 2019. In vitro and in vivo evidence that quercetin protects against diabetes and its complications: a systematic review of the literature. Biomed. Pharmacother. 109, 1085–1099. https://doi.org/10.1016/j.biopha.2018.10.130.

Shirai, T., Shichi, Y., Sato, M., Tanioka, Y., Furusho, T., Ota, T., Tadokoro, T., Suzuki, T., Kobayashi, K., Yamamoto, Y., 2016. High dietary fat-induced obesity in Wistar rats and type 2 diabetes in nonobese Goto-Kakizaki rats differentially affect retinol binding protein 4 expression and vitamin A metabolism. Nutrition research (New York, N.Y.), 36(3), 262–270. https://doi.org/10.1016/j.nutres.2015.11.018.

Suvarna, K., Layton, C., Bancroft, J., 2013. The Hematoxylin and eosin, Connective and mesenchymal tissues with their stains, Immunohistochemical techniques and Transmission electron microscopy. Bancroft's Theory and Practice of Histological Techniques,. Churchill Livingstone Elsevier, Oxford.

Tanaka, M., Yamada, S., Iwasaki, Y., Sugishita, T., Yonemoto, S., Tsukamoto, T., Fukui, S., Takasu, K., Muso, E., 2009. Impact of obesity on IgA nephropathy: comparative ultrastructural study between obese and non-obese patients. Nephron Clin. Pract. 112 (2), c71–c78. https://doi.org/10.1159/000213084.

Terauchi, Y., Takamoto, I., Kubota, N., Matsui, J., Suzuki, R., Komeda, K., Hara, A., Toyoda, Y., Miwa, I., Aizawa, S., Tsutsumi, S., Tsubamoto, Y., Hashimoto, S., Eto, K., Nakamura, A., Noda, M., Tobe, K., Aburatani, H., Nagai, R., Kadowaki, T., 2007. Glucokinase and IRS-2 are required for compensatory beta cell hyperplasia in response to high-fat diet-induced insulin resistance. J. Clin. Invest. 117, 246–257. https://doi.org/10.1172/JCI17645.

Ternacle, J., Wan, F., Sawaki, D., Surenaud, M., Pini, M., Mercedes, R., Ernande, L., Audureau, E., Dubois-Rande, J.L., Adnot, S., Hue, S., Czibik, G., Derumeaux, G., 2017. Short-term high-fat diet compromises myocardial function: a radial strain rate imaging study. Eur. Heart J. Cardiovasc. Imaging. 18 (11), 1283–1291. https://doi.org/10.1093/ehjci/jew316.

Vijayakumar, R.S., Surya, D., Nalini, N., 2004. Antioxidant efficacy of black pepper (Piper nigrum L.) and piperine in rats with high fat diet induced oxidative stress. Redox Rep 9 (2), 105–110. https://doi.org/10.1179/135100042250004742.

Yang, D.K., Kang, H.S., 2018. Anti-diabetic effect of cotreatment with quercetin and resveratrol in streptozotocin-induced diabetic rats. Biomol Ther. 26 (2), 130–138. https://doi.org/10.4062/biomolther.2017.254.

Yang, P., Xiao, Y., Luo, X., Zhao, Y., Zhao, L., Wang, Y., Wu, T., Wei, L., Chen, Y., 2017. Inflammatory stress promotes the development of obesity-related chronic kidney disease via CD36 in mice. J. Lipid Res. 58 (7), 1417–1427.

Yi, X., Cai, X., Wang, S., Xiao, Y., 2020. Mechanisms of impaired pancreatic β–cell function in high–fat diet–induced obese mice: the role of endoplasmic reticulum stress. Mol. Med. Rep. 21 (5), 2041–2050. https://doi.org/10.3892/mmr.2020.11013.

Zhang, X.Y., Guo, C.C., Yu, Y.X., Xie, L., Chang, C.Q., 2020. Establishment of high-fat diet-induced obesity and insulin resistance model in rats. J. Peking Univ., Health Sci. 52 (3), 557–563. https://doi.org/10.19723/j.issn.1671-167X.2020.03.024.

Zhang, X., Cui, Y., Fang, L., Li, F., 2008. Chronic high-fat diets induce oxide injuries and fibrogenesis of pancreatic cells in rats. Pancreas 37 (3), e31–e38.

Zhang, R., Yu, Y., Deng, J., Zhang, C., Zhang, J., Cheng, Y., Luo, X., Han, B., Yang, H., 2016. Sesamin ameliorates high-fat diet-induced dyslipidemia and kidney injury by reducing oxidative stress. Nutrients 8 (5), 276. https://doi.org/10.3390/nu8050276.

Zoccali, C., Vanholder, R., Massy, Z.A., Ortiz, A., Sarafidis, P., Dekker, F.W., Fliser, D., Fouque, D., Heine, G.H., Jager, K.J., Kanbay, M., Mallamaci, F., Parati, G., Rossignol, P., Wiecek, A., London, G., 2017. European renal and cardiovascular medicine (EURECA-m) working group of the european renal association – European dialysis transplantation association (ERA-EDTA). The systemic nature of CKD. Nat. Rev. Nephrol. 13 (6), 344–358. https://doi.org/10.1038/nrneph.2017.52.